Application of Active Noise Control for Reducing Snore

Sreeram R. Chakravarthy and Sen M. Kuo

Acoustics and Vibration Center
Department of Electrical Engineering
Northern Illinois University, DeKalb, IL 60115

Abstract:
This paper presents an application of active noise control (ANC) for reducing snoring noise. The proposed snore ANC system can be installed on a traditional headboard, thus has potential benefits in retrofit, convenience, and is unobtrusive. Six snore ANC structures were developed using three different filtered-x least mean square (FXLMS) algorithms to achieve better performance with lower computational complexity and overall system cost. Real-time experiments using a twin-size headboard and snore samples show a reasonable size of quiet zone with satisfactory performance achieved with a low-cost ANC system.

1. Introduction

Snoring is a prominent problem in modern society. The annoying intermittent nature of snoring disrupts the sleep of the bed partner, causing stress and social nuisance. Snoring volumes can reach high levels (90-100 dB) hence chronic exposure to high-level snoring is known to cause unilateral noise-induced hearing loss to a bed partner [1]. The sleep disruption has been linked to excessive daytime sleepiness of the snorer and his/her bed partner. This can result in loss of productivity in the work environment and lead to occupational accidents, or even reduce one's ability to safely operate a car.

For low-frequency snoring noise, passive methods such as earmuffs or earplugs are either ineffective or uncomfortable to wear during sleep. Therefore, the ANC systems [2, 3] based on the principle of superposition to attenuate low-frequency noise using secondary anti-noise of the same magnitude but opposite phase, have become a potential technique for reducing this annoying noise.

In this paper, we propose to reduce the snoring noise level at the snorer's bed partner's head location based on ANC techniques. To make this system more convenient and comfortable to use, the microphones and loudspeakers are mounted on the headboard. To improve system performance, we use two secondary loudspeakers and two error microphones; however, we can mix the reference signals and split the control signal for reducing algorithm complexity and system cost. Real-time experiments show this is an effective technique to create a quiet zone that allows head movement in a reasonable range by using a low-cost, single-channel ANC system.

2. Analysis of Snore Signals

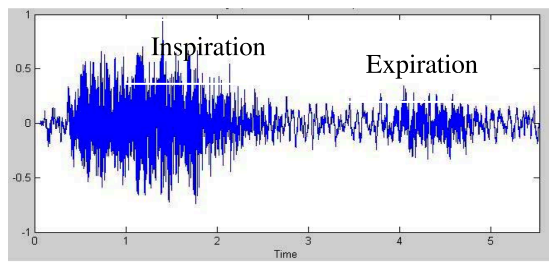

Figure 1 Waveform of a typical snore signal.

A snore is generated due to vibrations of the soft palate. This can be identified in the frequency spectrum as a large number of low-frequency harmonics [4]. This analysis proves important in the development of the snore ANC system, since it is relatively effective to generate a large quiet zone for low-frequency harmonics. A snore signal typically is comprised of two acoustic components: inspiration and expiration [5]. Figure 1 shows a period of time-domain snore waveform with the marked inspiration and expiration segments. This figure also shows an intermittent nature of typical snore signals.

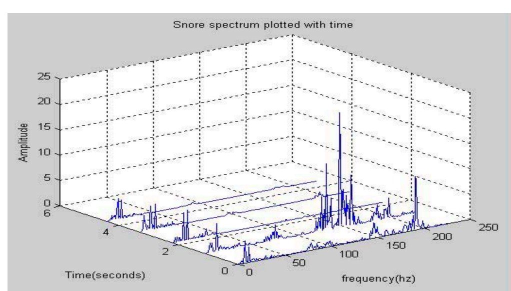

Figure 2 Three-dimensional display of snore spectra as a function of time and frequency.

Spectral content of the snore is an important factor to be considered in the development of the snore ANC systems. Figure 2 shows the spectra of snore plotted as a function of time A MATLAB program divides the snore signal shown in Figure 1 into 6 frames, and computes the spectrum for each frame. Figure 2 shows the snore signal has fast-changing spectral contents, and Figure 1 shows fast-changing of amplitude in time-domain waveform. These nonstationary characteristics make the snore ANC a very challenging real-world application.

3. ANC Algorithms and Simplified Configurations

The experimental setup for the snore ANC was built by modifying a twin-size headboard as shown in Figure 3, which is located inside an acoustic chamber. Two 6-1/2" loudspeakers are mounted on the headboard as the secondary source for generating canceling noise. Two error sensors are also mounted on the headboard to measure the residual noise. A model of a human torso called the KEMAR (Knowles electronics mannequin for acoustics research) is used as the bed partner who will be listening to the snoring noise. Two microphones installed inside the ear cavity of the KEMAR are used to evaluate the performance of the snore ANC at the ears of the bed partner.

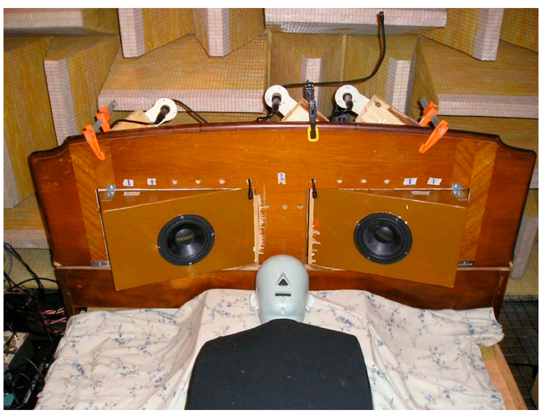

Figure 3 Experimental setup for the snore ANC.

The components not shown in include the primary noise source (snorer), which is simulated by a loudspeaker that is used to play the recorded snore. A reference microphone close to the noise source is used to pick up the snoring noise. A TMS320C32 floating-point digital signal processor board installed inside a personal computer is used to perform real-time experiments.

Snoring noises are nonstationary with fast-changing amplitude and spectral contents. Therefore, we have to use feedforward ANC systems with an upstream reference microphone that is close to the snorer. To provide convenience and comfort, we mounted error microphones on the headboard near both ears instead of asking the bed partner to wear wireless microphones. In order to create a quiet zone (centered at error microphones) that is large enough to cover the area surrounding bed partner's head, we need a single-reference/multiple-output FXLMS algorithm [6].

There are two error microphones mounted on the headboard to measure the residual noise components $e_1(n)$ and $e_2(n)$. The ANC system generates two canceling signals $y_1(n)$ and $y_2(n)$ using adaptive filters $W_1(z)$ and $W_2(z)$, respectively. The weight vectors are updated using the following 1x2x2 FXLMS algorithm [2]:

$$y_i(n) = \mathbf{w}_i^T(n)\mathbf{x}(n), \quad i = 1, 2 \tag{1}$$

$$\mathbf{w}_1(n+1) = \mathbf{w}_1(n) + \mu[e_1(n)\mathbf{x}(n) * \hat{s}_{11}(n) + e_2(n)\mathbf{x}(n) * \hat{s}_{21}(n)] \tag{2}$$

$$\mathbf{w}_2(n+1) = \mathbf{w}_2(n) + \mu[e_1(n)\mathbf{x}(n) * \hat{s}_{12}(n) + e_2(n)\mathbf{x}(n) * \hat{s}_{22}(n)] \tag{3}$$

Here, $\mathbf{w}_1(n)$ and $\mathbf{w}_2(n)$ are the weight vectors of the adaptive filters $W_1(z)$ and $W_2(z)$, respectively, μ is the adaptation step size that determines stability and speed of convergence, $\mathbf{x}(n)$ is the input signal vector, $\hat{s}_{11}(n)$ and $\hat{s}_{21}(n)$ are the estimated impulse responses of the secondary paths from loudspeaker #1 to the two microphones, $\hat{s}_{12}(n)$ and $\hat{s}_{22}(n)$ are from loudspeaker #2 to the two error microphones.

To simplify the algorithm complexity, we use a single error microphone or mix two analog signals sensed by two error microphones and digitize the mixer output to form $e(n)$. A new 1x2x1 FXLMS algorithm expressed as:

$$\mathbf{w}_1(n+1) = \mathbf{w}_1(n) + \mu[e(n)\mathbf{x}(n) * \hat{s}_1(n)] \tag{4}$$

$$\mathbf{w}_2(n+1) = \mathbf{w}_2(n) + \mu[e(n)\mathbf{x}(n) * \hat{s}_2(n)]\,. \tag{5}$$

Here, $\hat{s}_1(n)$ and $\hat{s}_2(n)$ are the estimated impulse responses of the secondary paths from two loudspeakers to the error microphone. Two canceling signals $y_1(n)$ and $y_2(n)$ are generated by adaptive filters $W_1(z)$ and $W_2(z)$, respectively, using equation (2).

Finally, we use only one adaptive filter $W(z)$ to generate a single canceling signal $y(n)$. This simple 1x1x1 FXLMS algorithm is illustrated in Figure 4, where $d(n)$ is the primary noise to be canceled, $e(n)$ is the error signal measured by the error sensor (or mixed two error sensors), and $\hat{S}(z)$ is the model of the secondary path $S(z)$, which can be obtained by off-line modeling. The 1x1x1 FXLMS algorithm is expressed as:

$$y(n) = \mathbf{w}^T(n)\mathbf{x}(n) \tag{6}$$

$$\mathbf{w}(n+1) = \mathbf{w}(n) + \mu e(n)\mathbf{x}(n) * \hat{s}(n)\,, \tag{7}$$

where $\mathbf{w}(n)$ is the weight vector of the adaptive filter, and $\hat{s}(n)$ is the estimated impulse response of the secondary path $S(z)$.

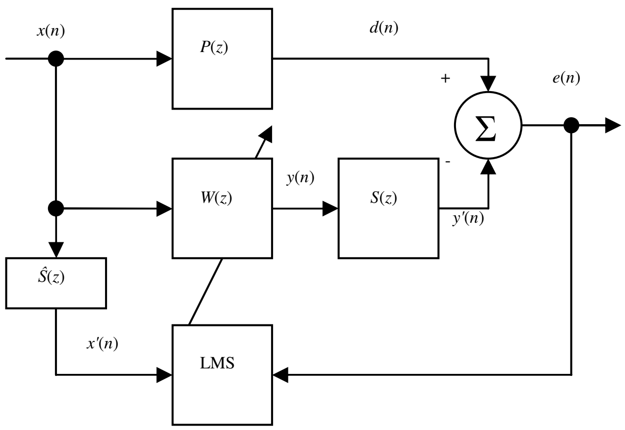

Figure 4 A feedforward 1x1x1 FXLMS algorithm.

The complexity of these three FXLMS algorithms in terms of the number of multiplications, additions, input channels, and output channels is summarized in Table 1. In this table, we assume the length of adaptive filters is L, and the length of the secondary path estimates is M. The input channel consists of the microphone, the preamplifier, the antialiasing filter, and the A/D converter; and the output channel contains the D/A converter, the smoothing filter, and the power amplifier.

Table 1 Complexity of FXLMS algorithms.

Algorithm	Multiply	Add	Input channel	Output channel
1x1x1	$2L+M+1$	$2L+M-2$	2	1
1x2x1	$4L+2M+2$	$4L+2M-4$	2	2
1x2x2	$4L+4M+2$	$6L+4M-8$	3	2

Table 2 Six snore ANC structures.

Conf.	Secondary sources	Error sensor	Algor.
#1	1	1	1x1x1
#2	1	2 (error sensor outputs are mixed)	1x1x1
#3	2 (secondary sources are driven by the same anti-noise)	1	1x1x1
#4	2 (secondary sources are driven by the same anti-noise)	2 (error sensor outputs are mixed)	1x1x1
#5	2	1	1x2x1
#6	2	2	1x2x2

It is important to note that with increased computational power and decreased cost of digital signal processors, the major overall system cost depends on the number of input/output channels. This paper develops and evaluates six different ANC structures with three FXLMS algorithms. These structures and their associated algorithms used for experiments are summarized in Table 2. These six structures use the same single reference microphone mounted on the headboard close to the snorer.

The ANC structures #1, #2, #3, and #4 use the simplest 1x1x1 FXLMS algorithm illustrated in Figure 4. In structures #2 and #4, two error microphone outputs are blended and then converted to a digital error signal $e(n)$ for the 1x1x1 FXLMS algorithm. In structures #3 and #4, the adaptive filter output $y(n)$ is split into two signals to drive the two loudspeakers shown in Figure 3.

4. Real-Time Experiments

Real-time experiments were performed on the TMS320C32 development system using the setup shown in Figure 3. Digital snore signals [7] were recorded on a digital audio tape and played on the loudspeaker to simulate the snorer. ANC structures #2 and #4 improve coherence by summing output from the two error sensors, thus achieving better performance.

To satisfy causality constraint, we need a longer distance between the snorer to his/her bed partner, a shorter distance between the reference microphone and the snorer, and a shorter distance between the secondary loudspeaker and the ear of bed partner. One possible solution is to extend the reference microphone and the secondary loudspeakers out from the headboard, or to use a larger size bed to provide adequate distance between the snorer and his/her bed partner.

The spectra of the residual snores picked up by the microphones inside the ears of the KEMAR for different ANC configurations were estimated and recorded. The plots show the spectra before and after ANC for all six ANC configurations and are detailed in [8]. In this section, we only show the best results achieved by structures #4.

Figures 4 and 5 show the spectra of the snore before and after ANC at the left and right ears of the KEMAR, respectively. The average reduction of the snore noise level is in the range of 5-10 dB.

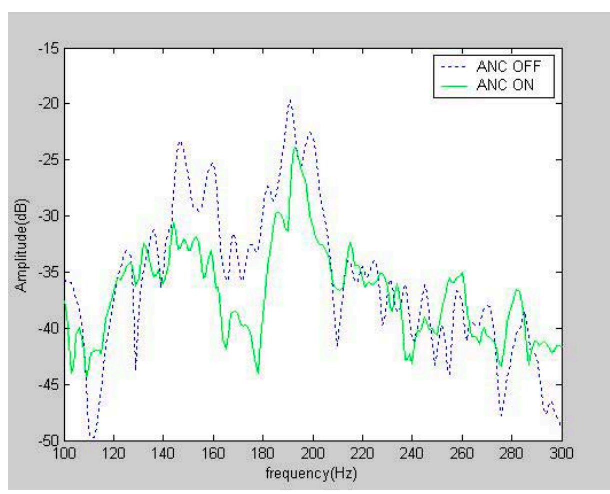

Figure 4 Spectra of snore at the left ear of KEMAR before and after ANC.

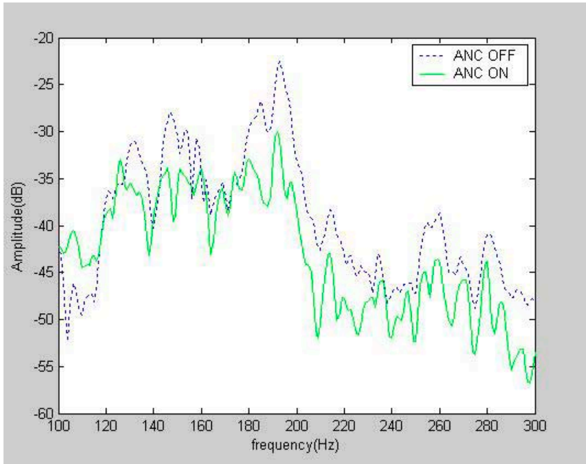

Figure 5 Spectra of snore at the right ear of KEMAR before and after ANC.

A mapping of the quiet zone produced by various snore ANC configurations (with the error microphones mounted on the headboard) shows the performance of the ANC system surrounding the ears of the bed partner. Since a snore is intermittent and lasts for a very short duration, quiet zone mapping using a snore would be very difficult and inaccurate. Hence a stationary colored noise with similar spectral characteristics as the snore was used to map the quiet zone. The generated color noise was reproduced by the loudspeaker that was originally used to play the snore.

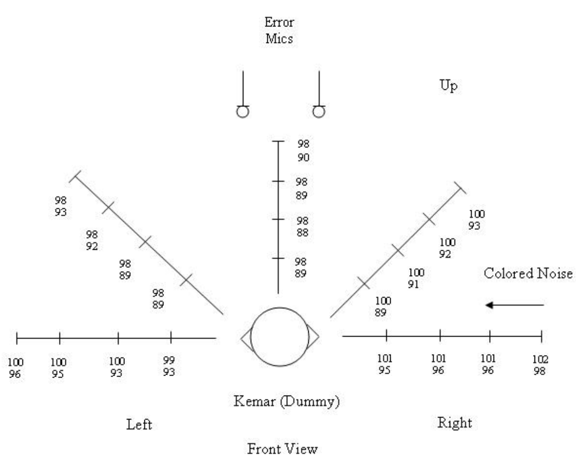

Figure 6 Quiet zone of the snoring ANC using the structures #4.

A Bruel and Kjaer sound level meter was used to measure the sound pressure levels in dB at various points surround the KEMAR before and after the ANC system was turned on. Figure 6 shows an example of quiet zone achieved by ANC structures #4. The measurement points are separated by 2 inches so as to cover a radius of 8 inches around the KEMAR. Measurements are made in five directions, upward from the face of the KEMAR, at a 45° angle upward on both sides of the head, and in the left and right directions of the ears. The values on the top at every location indicate the sound pressure level in dB without ANC, and the values at the bottom indicate the sound pressure level with the ANC. The results of quiet zone mapping with different configurations are detailed in [8].

The FXLMS algorithm minimizes the residual noise picked up by the error sensor, thus it creates a quiet zone centered at the error sensor. However, the objective of a snore ANC system is to reduce the noise at the ears. Real-time experiments show that the achievable noise reduction at the ears (Figures 4 and 5) is less than that at the error sensors. One possible solution is to ask the sleeper to wear a headband with two flat, wireless error microphones close to ears. However, this not only reduces the convenience and comfort of using the snore ANC system, but also creates a difficult problem of time-varying secondary paths due to the movement of error microphones.

5. Conclusions

This paper presented a new ANC application for reducing snore levels at the bed partner location. The experimental setup is based on a twin-size bed, was built with both error microphones and secondary loudspeakers installed on the headboard. Six snore ANC structures using three different FXLMS algorithms were developed and extensively tested using real-time experiments. Experimental results showed that the snore ANC system can reduce annoying snoring significantly and offers an unobtrusive and comfortable system on existing headboards.

References:

[1] G. M. Sardesai, A. K. W. Tan, and M. Fitzpatrick, "Noise-Induced Hearing Loss in Snorers and their Bed Partners," *J. Otolaryngology*, vol. 32, pp. 141-145, 2003.

[2] S. M. Kuo and D. R. Morgan, *Active Noise Control Systems: Algorithms and DSP Implementations*, John Wiley, 1996.

[3] S. M. Kuo and D. R. Morgan, Active Noise Control: A Tutorial Review, *Proc. of the IEEE,* vol. 8, pp. 943-973, June 1999.

[4] J. Schafer and W. Pirsig, "Digital Signal Analysis of Snoring Sounds in Children," *Int. Journal of Pediatric Otorhinolaryngology*, vol. 20, pp. 193-202, 1990.

[5] A. Cohen and A. Lieberman, "Analysis and Classification of Snoring Signals," in *Proc. ICASSP*, pp. 693-696, April 1986.

[6] D. R. Morgan, "An Analysis of Multiple Correlation Cancellation Loops with a Filter in the Auxiliary Path," *IEEE Trans. on Acoust. Speech Signal Processing*, vol. ASSP-28, pp. 454-467, Aug. 1980.

[7] Digitized wave files by Computer Audio Engineering, available from website: www.caeaudio.com.

[8] S. R. Chakrovorthy, *Active Snore Noise Control Systems*, M.S. Thesis, Northern Illinois University, Dec. 2005.